



## Structural nature of chemically inequivalent borons in the nonlinear optical material $\beta$ -BaB<sub>2</sub>O<sub>4</sub> studied using <sup>11</sup>B MAS NMR and <sup>11</sup>B single-crystal NMR

Woo Young Kim<sup>1</sup> and Ae Ran Lim<sup>1,2,\*</sup>

<sup>1</sup>Department of Carbon Fusion Engineering, Jeonju University, Jeonju 560-759, Korea

<sup>2</sup>Department of Science Education, Jeonju University, Jeonju 560-759, Korea

Received Nov 10, 2013; Revised Dec 09, 2013; Accepted Dec 18, 2013

**Abstract** Detailed information about the structural nature of three-coordinate borons in  $\beta$ -BaB<sub>2</sub>O<sub>4</sub> is obtained through <sup>11</sup>B MAS NMR and <sup>11</sup>B single-crystal NMR. The three-coordinate BO<sub>3</sub> of the two borons B(1) and B(2) in  $\beta$ -BaB<sub>2</sub>O<sub>4</sub> were distinguished. The spin-lattice relaxation time in the laboratory frame  $T_1$  for B(1) and B(2) slowly decreases with increasing temperature, whereas the spin-lattice relaxation time in the rotating frame  $T_{1\rho}$  for B(1) and B(2), which differs from  $T_1$ , is nearly constant. The B(1) and B(2) of the two types were distinguished by <sup>11</sup>B MAS NMR and <sup>11</sup>B single-crystal NMR.

**Keywords** Nonlinear optical property, Boron, MAS NMR, Single crystal NMR, Relaxation time

### Introduction

Nonlinear optical (NLO) materials have played an important role in laser science and technology. Among the nonlinear optical crystals, beta barium metaborate,  $\beta$ -BaB<sub>2</sub>O<sub>4</sub>, has shown good promise owing to its large second harmonic generation (SHG) coefficients [1]. In addition, borates have been

traditionally used in the glass industry. The developments in the fast evolving field of nanoscience and nanotechnology, where size and shape are crucial for determining the optoelectronic properties of materials, especially in the preparation of various  $\beta$ -BaB<sub>2</sub>O<sub>4</sub> nanostructures such as nanowires, nanorods, and nanotubes and studies on their SHG performance on the nanoscale, are noteworthy [2-5]. Recently, the anisotropy of the electrical and dielectric properties of  $\beta$ -BaB<sub>2</sub>O<sub>4</sub> single crystals has been reported and discussed [6, 7]. Further, the progress in large  $\beta$ -BaB<sub>2</sub>O<sub>4</sub> single crystal growth and the technique involved in growing these crystals have been reported [4, 8, 9].

The <sup>11</sup>B environments in  $\beta$ -BaB<sub>2</sub>O<sub>4</sub> single crystals were obtained through <sup>11</sup>B nuclear magnetic resonance (NMR) [10]. The <sup>11</sup>B NMR work reported two B sites with very similar quadrupolar coupling constants and asymmetry parameters:  $e^2qQ/h = 2.455$  MHz and  $\eta = 0.684$  for B(1), and  $e^2qQ/h = 2.486$  MHz and  $\eta = 0.644$  for B(2). The quadrupolar coupling constants for <sup>135</sup>Ba and <sup>137</sup>Ba were  $e^2qQ/h = 14.9$  MHz and  $e^2qQ/h = 22.8$  MHz, respectively [11]. Recently, the <sup>11</sup>B spin-lattice relaxation time in the laboratory frame  $T_1$  in  $\beta$ -BaB<sub>2</sub>O<sub>4</sub> crystals was reported as a function of temperature [12].

Solid-state NMR spectroscopy provides invaluable

\*Address correspondence to: Ae Ran Lim, Department of Science Education, Jeonju University, Jeonju 560-759, Korea, Tel: +82-(0)63-220-2514; Fax:+82-(0)63-220-2053; E-mail: aeranlim@hanmail.net

information on the local environment around the nucleus of interest.  $^{11}\text{B}$  magic angle spinning (MAS) NMR and single-crystal  $^{11}\text{B}$  NMR were employed to characterize the  $^{11}\text{B}$  environments. In this research, the structural nature of three-coordinate  $\text{BO}_3$  of two types in  $\beta\text{-BaB}_2\text{O}_4$  was studied using  $^{11}\text{B}$  MAS NMR and single-crystal  $^{11}\text{B}$  NMR. In order to obtain detailed information about the environments of the two borons, it is necessary to measure the spin-lattice relaxation times in the rotating frame,  $T_{1\rho}$ , of  $^{11}\text{B}$  nuclei. Moreover, this information can be used to work out guidelines for investigating and developing NLO materials.

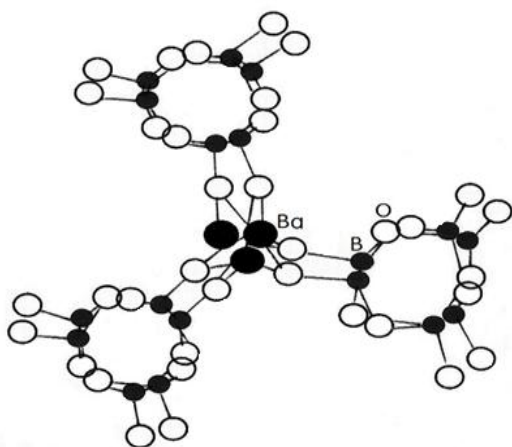


**Figure 1.** Linkage of  $\text{Ba}_3[\text{B}_3\text{O}_6]_6^{12-}$  rings with barium atoms in  $\beta\text{-BaB}_2\text{O}_4$ .

### Crystal structure

The composition of barium metaborate,  $\text{BaB}_2\text{O}_4$ , has two modifications for the crystal structure—high temperature ( $\alpha$ ) phase and low temperature ( $\beta$ ) phase—and the  $\beta\text{-BaB}_2\text{O}_4$  crystal is known to exhibit nonlinear optical properties. The crystal structure of the  $\beta\text{-BaB}_2\text{O}_4$  is trigonal (space group  $R3c$ ) with six formula units in a unit cell having dimensions of  $a = 8.380 \text{ \AA}$  and  $\alpha = 96.65^\circ$  [13–15]. There are two  $\text{Ba}_3(\text{B}_3\text{O}_6)_2$  molecules in a primitive unit cell, as shown in Fig. 1 [16]. Their lattice constants are of two distinct  $(\text{B}_3\text{O}_6)^{3-}$  planar groups that are oriented perpendicular to the  $c$ -axis and that alternate in pairs along the  $c$ -axis. These groups are laterally separated by the  $\text{Ba}^{2+}$  ions. The crystal has four crystallographically inequivalent sites for oxygen, two crystallographically inequivalent sites for boron,

and one site for barium. There are two types of boron atoms, B(1) and B(2), that form different boron-oxygen rings, and therefore lie at chemically inequivalent sites [17]. The nearest-neighbor, B(1)-O bond lengths have an average distance of  $1.377 \text{ \AA}$ , whereas the B(2)-O bond lengths have an average distance of  $1.371 \text{ \AA}$ .

### Experimental method

Single crystals of  $\beta\text{-BaB}_2\text{O}_4$  were grown by the modified flux method at CASIX in China. The crystal was cut along two crystallographic  $a$ -axis- and  $c$ -axis, and along another  $b$ -axis perpendicular to these axes. The single-crystal NMR signals of the  $^{11}\text{B}$  nuclei in  $\beta\text{-BaB}_2\text{O}_4$  were measured using a Bruker 400 FT NMR spectrometer at the Korea Basic Science Institute. The static magnetic field was  $9.4 \text{ T}$ , and the central radio frequency was set at  $\omega_0/2\pi = 128.34 \text{ MHz}$  for the  $^{11}\text{B}$  nucleus. The spin-lattice relaxation time in the laboratory frame,  $T_1$ , was measured by applying a pulse sequence of  $\pi/2-t-\pi/2$ . The nuclear magnetizations  $M(t)$  of the  $^{11}\text{B}$  nuclei at time  $t$  after the  $\pi/2$  pulse were determined from each saturation recovery sequence following the pulse. The width of the  $\pi/2$  pulse was  $0.5 \text{ \mu s}$  for  $^{11}\text{B}$ .

In addition, in order to obtain the spin-lattice relaxation time in the rotating frame,  $T_{1\rho}$ , solid-state  $^{11}\text{B}$  MAS NMR experiments were performed using a Bruker 400 FT MHz NMR spectrometer.  $^{11}\text{B}$  MAS NMR experiment was performed at the Larmor frequency of  $128.34 \text{ MHz}$ . The samples were placed in powder form in the  $4 \text{ mm CP/MAS}$  probe. The MAS rate was set at  $10 \text{ kHz}$  for  $^{11}\text{B}$ , to minimize spinning sideband overlap. The width of the  $\pi/2$  pulse for  $^{11}\text{B}$  was  $5 \text{ \mu s}$ , corresponding to the spin-locking field strength of  $50 \text{ kHz}$ . The measurement of  $^{11}\text{B}$  spin-lattice relaxation time in the rotating frame,  $T_{1\rho}$ , was performed by applying  $^{11}\text{B}$  spin-locking pulses.

### Experimental results and discussion

We describe the recovery laws for the quadrupole relaxation process in the  $^{11}\text{B}$  ( $I = 3/2$ ) nuclear-spin

system; these are described by non-exponential functions. The temperature dependence of the relaxation time is indicative of fluctuations in the electric-field-gradient (EFG) tensor, driven by a thermally activated motion. The saturation recovery traces for the central line of  $^{11}\text{B}$  with dominant quadrupole relaxation can be represented as a combination of two exponential functions [18, 19]:

$$[M(\infty) - M(t)]/M(\infty) = 0.5[\exp(-2W_1t) + \exp(-2W_2t)] \quad (1)$$

where  $M(\infty)$  is the thermal equilibrium magnetization and  $M(t)$  is the nuclear magnetization at time  $t$ ;  $W_1$  and  $W_2$  are the transition probabilities for  $\Delta m = \pm 1$  and  $\Delta m = \pm 2$ , respectively. Thus, the relaxation time is given by  $T_1 = 5/[2(W_1 + 4W_2)]$ .

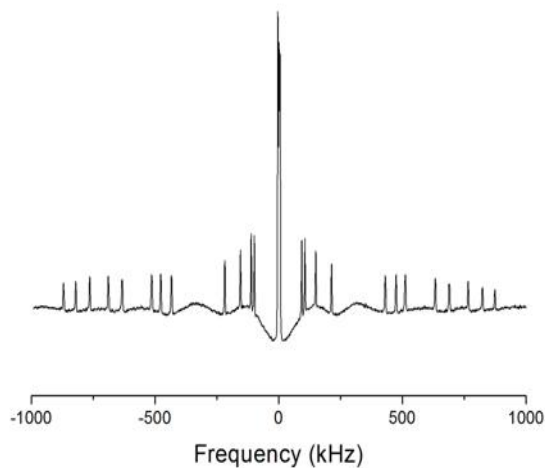


**Figure 2.**  $^{11}\text{B}$  NMR spectra of a  $\text{BaB}_2\text{O}_4$  single crystal at room temperature. The static magnetic field is parallel to the  $a+50^\circ$ -axis in the  $ac$ -plane.

The spin-lattice relaxation times in the rotating frame  $T_{1\rho}$  for  $^{11}\text{B}$  in  $\beta\text{-BaB}_2\text{O}_4$  were measured at several temperatures. The  $T_{1\rho}$  values were obtained by Fourier transformation of the FID following the end of spin locking and by repetition of the experiments for various periods of time  $t$ . All the magnetization traces obtained for  $^{11}\text{B}$  were fitted with the following single exponential function [20, 21]:

$$M(t)/M(0) = \exp(-Wt) \quad (2)$$

The spin-lattice relaxation time in the rotating frame  $T_{1\rho}$  is given by  $T_{1\rho} = 1/W$ .

Usually, the  $^{11}\text{B}$  NMR spectrum of  $\beta\text{-BaB}_2\text{O}_4$  crystals consists of a central line and two satellite lines. Here, the resonance lines were observed when the magnetic field was applied along the  $a+50^\circ$ -axis in the  $ac$ -plane of the crystal. Therefore, if the local symmetry around the boron atoms is not cubic, a boron atom gives three resonance lines, and 12 boron atoms in a  $\text{BaB}_2\text{O}_4$  unit cell gives a total of 24 satellite lines, as shown in Fig. 2. The three central resonance lines for the  $^{11}\text{B}$  nucleus are caused by the magnetically inequivalent sites and the chemically inequivalent sites. Here, the two central resonance lines for B(2) are due to the magnetically inequivalent but chemically equivalent sites, as shown in the inset in Fig. 3. Consequently, the  $^{11}\text{B}$  spectrum indicates the presence of two types of chemically inequivalent  $^{11}\text{B}$  nuclei, designated B(1) and B(2) [10]. The zero point of the horizontal axis corresponds to the resonance frequency of the  $^{11}\text{B}$  nucleus (i.e., 128.34 MHz). The magnitudes of the quadrupole parameters of  $^{11}\text{B}$  nuclei are of the order of MHz, so usually the central resonance lines are split and shifted. The separation between the resonance lines is independent of temperature for both B(1) and B(2). There is no variation in the splitting of the  $^{11}\text{B}$  resonance lines with temperature, indicating that the EFG at the B sites remains unchanged, which in turn means that the neighboring atoms of the  $^{11}\text{B}$  nuclei are not displaced when the temperature is varied.

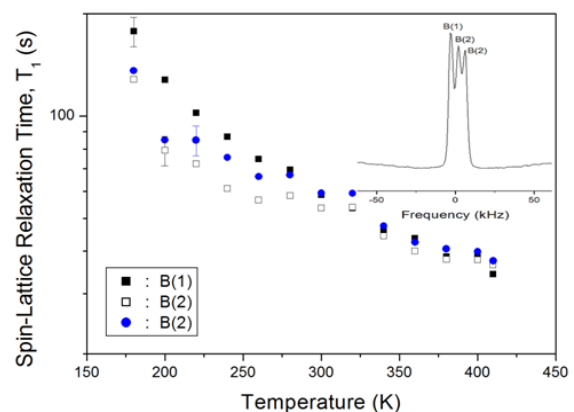


**Figure 3.** Temperature dependences of the spin-lattice relaxation time,  $T_1$ , of  $^{11}\text{B}$  in a  $\text{BaB}_2\text{O}_4$  single crystal (inset:  $^{11}\text{B}$  NMR central lines indicate the presence of two types of chemically inequivalent  $^{11}\text{B}$  nuclei, designated B(1) and

B(2)).

The nuclear magnetization recovery curves for the central lines of  $^{11}\text{B}$  were obtained by measuring the nuclear magnetization after applying saturation pulses.  $T_1$  was determined directly from the slope of a plot of  $\log [M(\infty) - M(t)]/M(\infty)$  versus time  $t$ . It is very well known that the relaxation time  $T_1$  can only be defined if the time dependence of the magnetization can be described by the two exponential relaxation functions of Eq. (1). Of course, one might introduce a useful combination of the transition probabilities  $W_1$  and  $W_2$  and explain that the introduction of this constant is reasonable because it leads to the correct relaxation time  $T_1 = 1/(2W_1)$  when  $W_1 = W_2$ , where a single exponential relaxation function can be derived from Eq. (1). The temperature dependence of the spin-lattice relaxation time in the laboratory frame  $T_1$  of  $^{11}\text{B}$  NMR is shown in Fig. 3. The relaxation times of the three-coordinated B(1) and three-coordinated B(2) can be distinguished. The value of  $T_1$  decreases slowly with increasing temperature, and  $T_1$  values for B(1) and B(2) follow a similar trend. Here, the values of  $T_1$  for  $^{11}\text{B}$  are long (30~200 s).

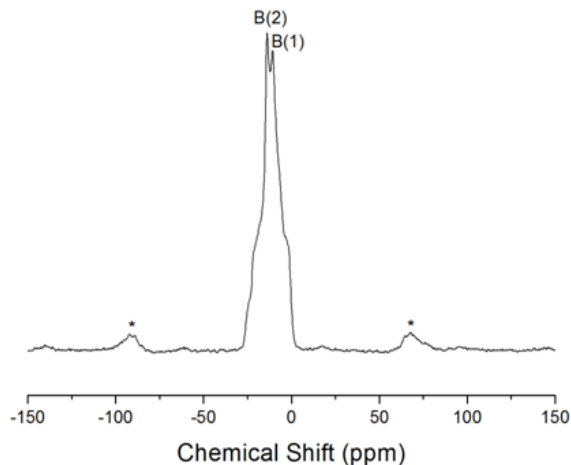


**Figure 4.**  $^{11}\text{B}$  MAS NMR spectrum at room temperature (B(1) and B(2) are three-coordinate  $\text{BO}_3$ ).

On the other hand, the structural analysis of the  $^{11}\text{B}$  in  $\beta\text{-BaB}_2\text{O}_4$  was carried out using the solid-state NMR method. The  $^{11}\text{B}$  MAS NMR spectrum of  $\beta\text{-BaB}_2\text{O}_4$  at room temperature is shown in Fig. 4. Overlapping the resonances at  $-13.82$  ppm and  $-10.77$  ppm are the

resonances from the trigonal  $\text{BO}_3$  groups. The  $^{11}\text{B}$  MAS NMR spectrum consists of two peaks at chemical shifts of  $\delta = -13.82$  ppm and  $-10.77$  ppm. The spinning sidebands are marked with asterisks. There are two types of boron atoms. The signals at chemical shifts of  $-13.82$  ppm and  $-10.77$  ppm are assigned to the trigonal  $\text{BO}_3$  (B(1)) and trigonal  $\text{BO}_3$  (B(2)) groups, respectively. The  $^{11}\text{B}$  spectrum obtained at room temperature indicates the presence of two types of chemically inequivalent  $^{11}\text{B}$  nuclei, designated B(1) and B(2). The intensity ratio is associated with the chemically inequivalent positions of B atoms in the unit cell [5], and the intensities for B(1) and B(2) are very similar.

The  $^{11}\text{B}$  spin-lattice relaxation times in the rotating frame,  $T_{1\rho}$ , were measured at several temperatures of  $\beta\text{-BaB}_2\text{O}_4$ . The nuclear magnetization recovery traces obtained for B(1) and B(2) are described by the following single exponential function,  $M(t) = M(\infty)\exp(-t/T_{1\rho})$  [19]; the recovery traces showed a single exponential decay at all temperatures. The slopes of the recovery traces are nearly same for each temperature. The temperature dependence of the  $^{11}\text{B}$  spin-lattice relaxation time in the rotating frame,  $T_{1\rho}$ , is shown in Fig. 5. The  $T_{1\rho}$  values of the three-coordinate B(1) and three-coordinate B(2) show similar trends, and that of B(1) is longer than that of B(2). The  $T_{1\rho}$  values for B(1) and B(2) are short (0.05~0.2 ms).

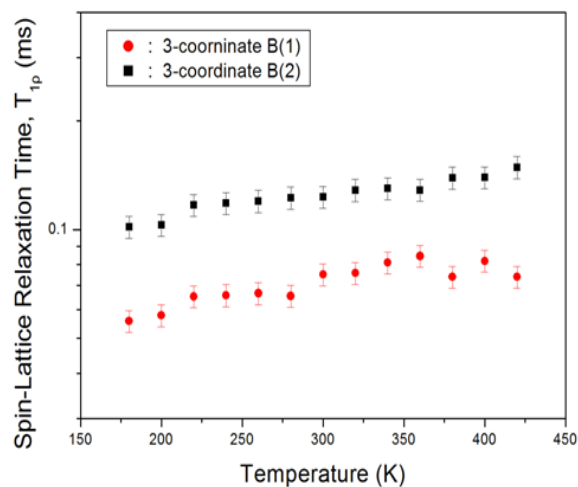


**Figure 5.** Temperature dependences of the spin-lattice relaxation time in the rotating frame,  $T_{1\rho}$ , of three-coordinate B(1) and three-coordinate B(2) in

$\beta$ -BaB<sub>2</sub>O<sub>4</sub>.

### Conclusion

<sup>11</sup>B MAS NMR spectroscopy is a well-established analytical tool for investigating several aspects of the diverse structural chemistry of boron.  $T_{1\rho}$  is affected by slower molecular motions as compared with  $T_1$ , and so the  $T_{1\rho}$  measurements provide additional information that can be used for a more reliable check on various models of motions.  $T_1$  slowly decreases with increasing temperature, whereas  $T_{1\rho}$ , which differs from  $T_1$ , is nearly constant with temperature. The value of  $T_1$  is very different from that of  $T_{1\rho}$ ;  $T_1 \sim 50$  s and  $T_{1\rho} \sim 0.1$  ms at room temperature. The ratio between the spin-lattice relaxation times in the laboratory frame,  $T_1$ , and in

the rotating frame,  $T_{1\rho}$ , is  $T_1/T_{1\rho} \approx 5 \times 10^5$ .  $T_{1\rho}$  for three-coordinated B(1) and for three-coordinate B(2) follow similar trends. Also, the  $T_{1\rho}$  value of B(2) is shorter than that of B(1). These results are consistent with the boron-oxygen distances of B(1)–O (1.377 Å) and B(2)–O (1.371 Å) [5].

The B(1) and B(2) of the two types were distinguished by <sup>11</sup>B MAS NMR and single-crystal <sup>11</sup>B NMR. No significant changes were seen in the  $T_{1\rho}$  at boron nuclei in  $\beta$ -BaB<sub>2</sub>O<sub>4</sub>. Thus, the local symmetry around the <sup>11</sup>B atoms is insensitive with respect to changes in temperature.

### Acknowledgements

This research was supported by the Basic Science Research Program through the National Research Foundation of Korea (NRF) funded by the Ministry of Education, Science and Technology (2012001763).

### References

1. C.T. Chen, B.C. Wu, A.D. Jiang, and G.M. You, *Sci. Sin. B* **18**, 235 (1985).
2. J. Hu, T.W. Odom, and C.M. Lieber, *Acc. Chem. Res.* **32**, 435 (1999).
3. Y.N. Xia, P.D. Yang, Y.G. Sun, Y.Y. Wu, B. Mayer, B. Gates, Y.D. Yin, F. Kim, and H.Q. Yan, *Adv. Mater* **15**, 353 (2003).
4. Q. Zhao, X. Zhu, X. Bai, H. Fan, and Y. Xie, *Eur. J. Inorg. Chem.* 1829 (2007).
5. J. Zhang, S. Liang, and G. He, *Chem. Letters* **38**, 500 (2009).
6. V. Trnovcova, P.P. Fedorov, A.E. Kokh, and I. Furar, *J. Phy. Chem. Solid* **68**, 1024 (2007).
7. V. Trnovcova, M. Kubliha, A. Kokh, P.P. Fedorov, and R.M. Zakalyukin, *Russian J. Electrochemistry* **47**, 531 (2011).
8. D. Perlov, S. Livneh, P. Czechowicz, A. Goldgirsh, and D. Loiacono, *Cryst. Res. Technol.* **46**, 651 (2011).
9. A.E. Kokh, T.B. Bekker, V.A. Vlezko, and K.A. Kokh, *J. Cryst. Growth* **318**, 602 (2011).
10. I.G. Kim and S.H. Choh, *J. Phys.: Condens. Matter* **11**, 8283 (1999).
11. A. Sutrisno, C. Lu, R.H. Lipson, and Y. Huang, *J. Phys. Chem. C* **113**, 21196 (2009).
12. A.R. Lim and I.G. Kim, *Solid State Commun.* **159**, 41 (2013).
13. S.F. Lu, M.Y. He, and J.L. Huang, *Acta. Phys. Sin.* **31**, 948 (1982).
14. J. Liebertz and S. Stahr, *Z. Kristallogr.* **165**, 91 (1983).
15. R. Frohlich, *Z. Kristallogr.* **168**, 109 (1984).
16. B.G. Wang, Z.P. Lu, E. W. Shi, and W.Z. Zhong, *Cryst. Res. Technol.* **33**, 275 (1998).
17. S.F. Lu, Z.X. Huang, and J.L. Huang, *Acta Cryst. C* **62**, i73 (2006).
18. J. Dolinsek, D. Arcon, B. Zalar, R. Pirc, R. Blinc, and R. Kind, *Phys. Rev. B* **54**, R6811 (1996)
19. A. Abragam, *The Principles of Nuclear Magnetism*, Oxford University Press, (1961).

20. E. Fukushima, S.B.W. Roeder, *Experimental Pulse NMR*, Addison-Wesley, Reading, MA, (1981).
21. P. Laszlo, *NMR of Newly Accessible Nuclei*, Academic, New York, (1993).